Title
Messenger RNA targeting to endoplasmic reticulum stress signalling sites.

Journal
Nature, 457(7230)

ISSN
0028-0836

Authors
Aragón, Tomás
van Anken, Eelco
Pincus, David
et al.

Publication Date
2009-02-01

DOI
10.1038/nature07641

Peer reviewed

Published as: *Nature*. 2009 February 5; 457(7230): 736–740.

mRNA Targeting to ER Stress Signaling Sites

Tomás Aragón[1,*,†], **Eelco van Anken**[1,*], **David Pincus**[1], **Iana M. Serafimova**[1], **Alexei V. Korennykh**[1], **Claudia A. Rubio**[1], and **Peter Walter**[1,2]

[1]Department of Biochemistry and Biophysics, University of California at San Francisco, San Francisco, California 94158-2517, USA.

[2]Howard Hughes Medical Institute, University of California at San Francisco, San Francisco, California 94158-2517, USA.

Abstract

Deficiencies in the protein folding capacity of the endoplasmic reticulum (ER) in all eucaryotic cells lead to ER stress and triggers the unfolded protein response (UPR)1–3. ER stress is sensed by Ire1, a transmembrane kinase/endoribonuclease, which initiates the non-conventional splicing of the mRNA encoding a key transcription activator, Hac1 in yeast or XBP-1 in metazoans. In the absence of ER stress, ribosomes are stalled on unspliced *HAC1* mRNA. The translational control is imposed by a base pairing interaction between the *HAC1* intron and the *HAC1* 5′ untranslated region (5′UTR)4. After excision of the intron, tRNA ligase joins the severed exons5,6, lifting the translational block and allowing synthesis of Hac1 from the spliced *HAC1* mRNA to ensue4. Hac1 in turn drives the UPR gene expression program comprising 7–8% of the yeast genome7 to counteract ER stress. We show here that upon activation, Ire1 molecules cluster in the ER membrane into discrete foci of higher-order oligomers, to which unspliced *HAC1* mRNA is recruited by means of a conserved bipartite targeting element contained in the 3′ untranslated region (3′UTR). Disruption of either Ire1 clustering or of *HAC1* mRNA recruitment impairs UPR signaling. The *HAC1* 3′UTR element is sufficient to target other mRNAs to Ire1 foci, as long as their translation is repressed. Translational repression afforded by the intron fulfills this requirement for *HAC1* mRNA. Recruitment of mRNA to signaling centers provides a new paradigm for the control of eukaryotic gene expression.

In vitro studies suggest that the information required for *HAC1* mRNA splicing is confined to the intron and the regions surrounding the splice junctions8. Surprisingly, *in vivo* splicing of *HAC1* mRNA was greatly diminished when its 3′UTR was replaced by the 3′UTRs of other yeast mRNAs, such as of *ACT1* (Fig. 1b) or *PGK1* (data not shown). Consistent with this finding, cells bearing a chimeric *hac1*-3′*act1* mutant gene expressed Hac1 protein at trace levels that were too low to mount a functional UPR and failed to grow in ER stress

---

[†]To whom correspondence should be addressed. e-mail: Tomas.Aragon@ucsf.edu.
[*]These authors contributed equally to this work.

conditions (Fig. 1b). Thus, the *HAC1* 3′UTR harbors an element important for *HAC1* mRNA splicing *in vivo*.

Mutational probing experiments (not shown) indicate that the *HAC1* 3′UTR contains a prominent, extended stem-loop (Fig. 1c). Interestingly, two short sequence motifs within the stem-loop are highly conserved among all *HAC1* orthologs identified; eight representatives are shown in Figure 1d. The sequence motifs map to opposite strands and are juxtaposed in the distal part of the stem, constituting a bipartite element (3′BE for 3′UTR Bipartite Element) (Fig. 1c, 3′BE in red).

To assess the importance of the 3′BE for *HAC1* mRNA splicing *in vivo*, we employed a splicing reporter (SpR) in which we replaced the first 648 nucleotides of the *HAC1* coding sequence in the first exon with that of GFP (Fig. 1a, green bar). This reporter allowed us to monitor the effect of 3′UTR mutations on mRNA splicing in cells that can mount a functional UPR, sustained by endogenous *HAC1* mRNA. The SpR mRNA was efficiently spliced upon UPR induction. By contrast, splicing was significantly diminished when the 3′BE (Δ3′BE) was deleted (Fig. 1e). Consistent with these results, deletion of the 3′BE in *HAC1* severely reduced *HAC1* mRNA splicing and impaired cell survival under ER stress conditions (Fig. 1e). Only residual splicing of endogenous *HAC1* mRNA occurred in the absence of the 3′BE, indicating that the 3′BE accounts in large part for the contribution of the 3′UTR to *HAC1* mRNA splicing. Insertion of a 64-nucleotide 3′UTR fragment containing the central portion of the stem including the 3′BE (Fig. 1d, enlarged on right) into the SpR bearing the *ACT1* 3′UTR restored splicing significantly (Fig. 1f).

To test whether the 3′UTR affects the ability of Ire1 endonuclease to bind or catalyze the cleavage of *HAC1* mRNA, we reconstituted the intron excision reaction *in vitro*. Ire1 cleaved *HAC1* mRNA with the same rate in the presence or absence of the 3′BE (Fig. 1g). Thus, the 3′BE is not required for splicing *in vitro*.

The importance of the 3′BE for *HAC1* mRNA splicing *in vivo* suggested it may serve to target the mRNA to sites in the cell where splicing takes place. To test this notion, we visualized Ire1 and *HAC1* mRNA *in vivo*, using the imaging constructs depicted in Figure 2a. For Ire1, we inserted a GFP or mCherry into the cytosolic portion of Ire1 adjacent to its transmembrane region. For *HAC1* mRNA, we inserted 16 copies of a U1A binding site into the 3′UTR downstream of the 3′BE. This mRNA can then be visualized by co-expression of a U1A-GFP fusion that docks to the U1A sites. Both Ire1 and *HAC1* mRNA imaging constructs fully restored growth of *ire1*Δ and *hac1*Δ (Fig. 2b) cells under ER stress. In the absence of stress, Ire1-GFP co-localized with the ER marked by Sec63-mCherry (Fig. 2c). The majority of $HAC1^{U1A}$ mRNA displayed a grainy signal dispersed throughout the cytosol (Fig. 2d), with a fraction of *HAC1* mRNA signal also found at the ER in agreement with previous observations9.

Induction of ER stress dramatically altered localization of both Ire1 and *HAC1* mRNA. The vast majority (82 ± 6%; see Methods) of Ire1 clustered into distinct foci localized both to the nuclear envelope and the cortical ER (Fig. 2c–e), in agreement with recent observations10. Excitingly, *HAC1* mRNA strongly co-localized (co-localization index (“CI”): 56 ± 10; see

Methods; Fig. 2e) with Ire1 in foci (Fig. 2d, arrowheads). This recruitment is specific, since control *PGK1*^{U1A} mRNA remained dispersed in the cytosol under ER stress conditions (Fig. 2f).

Clustering of mRNAs in cytosolic foci is not unprecedented. Several stresses, such as nutrient starvation, cause aggregation of untranslated mRNAs into processing bodies (P-bodies) where they are stored and/or degraded11. The Ire1/*HAC1* mRNA clusters however are distinct from P-bodies: Upon glucose depletion, Lsm1-mCherry clustered into P-bodies as reported12, and *HAC1* mRNA co-localized with Lsm1-mCherry in these P-bodies. By contrast, under ER stress conditions the Lsm1-mCherry did not co-localize with *HAC1* mRNA foci but remained dispersed throughout the cytosol (Fig. 2g). Thus, the Ire1/*HAC1* mRNA foci constitute novel sites of mRNA clustering in the cytosol that are specific for the UPR.

We next determined the role of each of the three key UPR players, Ire1, *HAC1* mRNA and tRNA ligase in organizing the foci. In *rlg1-100* cells bearing mutant tRNA ligase defective in UPR signaling, co-clustering of Ire1 and *HAC1* mRNA occurred normally (Fig. 2h). This result is consistent with the fact that cleavage of *HAC1* mRNA by Ire1 is not dependent on the subsequent ligation step5. Likewise, *HAC1* mRNA was not required for Ire1 clustering, as Ire1-GFP formed foci in *hac1*Δ cells (Fig. 2h and [ref 11]). Conversely, *HAC1* mRNA failed to form foci in *ire1*Δ cells (Fig. 2h). Thus, clustering of Ire1 in response to ER stress is epistatic to *HAC1* mRNA clustering.

Having established that *HAC1* mRNA is targeted to Ire1 foci in an ER stress-driven manner, we assessed the role of *HAC1* mRNA's 3′UTR in the process. To this end, we added the U1A visualization module to the SpR used in Figure 1e. The SpR^{U1A} mRNA containing a wild-type *HAC1* 3'UTR co-localized with Ire1-mCherry in foci (CI: 64 ± 20, Fig. 2i). By contrast, co-localization with Ire1 foci of the SpR^{U1A} mRNA lacking the 3'BE was minimal (CI: 4 ± 6, Fig. 2i) at levels comparable to the control *PGK1*^{U1A} mRNA (CI: 6 ± 4). Thus, the stem-loop structure in the 3′UTR of *HAC1* mRNA – with the 3′BE at its core – indeed serves as a targeting element that guides *HAC1* mRNA to Ire1 foci to allow splicing *in vivo* and cell survival under ER stress.

We next followed a time course of foci formation and downstream signaling upon induction of ER stress. Clustering of Ire1 into foci and recruitment into these foci of *HAC1* mRNA (Fig. 3a,b) or of SpR^{U1A} mRNA (Supplementary Fig. S1) correlated well with the onset of *HAC1* mRNA splicing (Fig. 3) and Hac1 protein production (Fig. 3c). These findings show that Ire1 and *HAC1* mRNA clustering is geared to rapidly transduce ER stress. Under conditions where ER stress builds up more gradually, the encounter of Ire1 and *HAC1*^{U1A} mRNA in foci likewise paralleled the signaling response, but at a slower pace (Supplementary Fig. S2). The synchronicity of Ire1/*HAC1* mRNA clustering and downstream signaling events underscores that the foci constitute functional mRNA splicing centers.

Ire1 clusters in only few ~3–10 foci per cell. Because yeast contains ~200–300 molecules of Ire1 per cell13, the foci are composed of a few tens of Ire1 molecules each, suggesting that

the foci harbor higher-order oligomers of Ire1. From the crystal structure of the Ire1 ER-luminal domain, we identified two separate dimerization interfaces that both are essential for optimal UPR signaling, suggesting that oligomerization is important for cells to mount a robust UPR14 (Fig. 3d). Accordingly, simultaneous disruption of both interfaces dramatically reduced *HAC1* mRNA splicing and cell growth under ER stress conditions, while the single interface disruptions, which still can form Ire1 dimers via one interface, displayed intermediate splicing and growth phenotypes (Fig. 3e). Disruption of either interface prevented foci formation (Fig. 3f, Supplementary Fig. S3, and [ref 10]), indicating that Ire1 oligomerization is the organizing principle for UPR signaling foci. Importantly, Ire1's inability to form foci impaired *HAC1*^{U1A} mRNA recruitment (Fig. 3f and Supplementary Fig. S3). Thus, when Ire1 fails to oligomerize, *HAC1* mRNA recruitment becomes rate limiting. In agreement, we found that artificially induced dimerization15 of Ire1 supported *HAC1* mRNA splicing and cell survival under ER stress conditions only to the level of the single interface mutants and did not support Ire1 foci formation (Supplementary Fig. S4). We conclude that robust Ire1 oligomerization and *HAC1* mRNA targeting serve to concentrate both key UPR components into foci to ensure efficient RNA processing and ER stress signaling.

HAC1 mRNA no longer is a substrate for Ire1 after removal of its intron, suggesting that the spliced *HAC1* mRNA should disengage from Ire1 foci and not be recruited again. Accordingly, SpR^{U1A} mRNA lacking the intron displayed reduced targeting to foci (CI: 17± 9) as compared to wild-type SpR^{U1A} mRNA (Fig. 4a, b), although not as dramatically reduced as when the 3′BE was deleted (Fig. 2i and Fig. 4b). In further support, over-expression of SpR^{U1A} mRNA containing the intron reduced splicing of endogenous *HAC1* mRNA, presumably by competitively saturating Ire1 after being targeted there, but not so when SpR^{U1A} mRNA lacked either the 3′BE or the intron (Fig. 4c). These observations suggest that the 3′BE alone is not sufficient for efficient targeting. In agreement, insertion of *HAC1*'s 3′UTR stem (Fig. 1c) into the 3′UTR of *PGK1* could not facilitate recruitment of this heterologous mRNA to Ire1 foci (Fig. 4d). Thus, the intron and 3'BE cooperate to effect *HAC1* mRNA targeting.

The intron keeps *HAC1* mRNA translationally silent (Fig. 1a), suggesting the possibility that translational repression may be key to *HAC1* targeting as in other targeting mechanisms, as observed for *ASH1* mRNA16. To test this hypothesis, we inserted a small stem loop into the 5′UTR of the *PGK1*^{U1A} mRNA to repress its translation ([ref 17] and Fig. 4e). Remarkably, when we expressed *PGK1*^{U1A} mRNA containing both the small stem loop in the 5′UTR and the *HAC1* 3′BE-containing stem in the 3′UTR, we found that this mRNA efficiently targeted to Ire1 foci (CI: 46 ± 11, Fig. 4f, h). Conversely, the corresponding mRNA lacking the 3′BE was not targeted (Fig. 4g, h). We conclude that the 3′BE-containing stem is both necessary and sufficient to target a heterologous mRNA to UPR-induced Ire1 foci, provided that its translation is on hold. Translational repression, therefore, is not only key to facilitate timely synthesis of Hac1 protein upon induction of the UPR, but is also integral to the targeting of *HAC1* mRNA to ER stress signaling centers.

Our results describe a first example of mRNA targeting as a central feature in a signaling pathway. *HAC1* mRNA is delivered to the site where it is processed as part of the main

switch regulating the UPR. The mRNA guidance mechanisms characterized to date serve other goals, such as delivery of mRNA to sites of storage or degradation17,18, or restricted distribution of the proteins they encode19–21. *HAC1* mRNA delivery to Ire1 foci has in common with other mRNA targeting mechanisms that it depends on a signal in the 3'UTR and on translational repression of the mRNA22. The mechanism of translational control of *HAC1* mRNA serves both to prevent translation of a functional transcription factor, when the UPR is off, and to allow the mRNA access to the splicing machine, which removes the intron to allow its translation, when the UPR is on. In this way, the targeting signal is inactivated when translation of *HAC1* mRNA resumes, even though the 3′BE remains present in the spliced mRNA.

The translational block in *S. cerevisiae* is exerted via a 16-base pairing interaction between sequences in the 252 nucleotide-long intron and the 5′UTR4. Most *HAC1* or XBP1 orthologs bear introns that are shorter (~20–26 nucleotides) and show no sequence complementarity to support 5′UTR/intron based translational blocks. It is conceivable that other means of translational repression come into play. For instance, the PERK-mediated general translational attenuation in response to ER stress23 could serve a functionally similar role in XBP-1 mRNA targeting in metazoans.

Our findings emphasize the role of Ire1 oligomers, rather than dimers, in UPR signaling. Early co-immunoprecipitation studies already provided evidence for oligomerization24, and the identification of two functionally important interfaces that link Ire1 luminal domains into linear filaments in the crystal lattice supports an attractive model by which neighboring Ire1 molecules are 'stitched' together by the binding of unfolded proteins in the ER lumen14. This model and the epistasis data in Figure 2h suggest that Ire1 foci formation is governed by self-organization. Over-expression of Ire1 caused an enlargement of the foci, but did not increase their number (not shown), suggesting that there is a limited number of nucleation sites per cell and that foci may arise at such predisposed sites at the ER membrane. Since *HAC1* mRNA recruitment occurs with amazing speed and efficiency (e.g., Fig. 3), one can further speculate that the 3'BE containing targeting signal may allow *HAC1* mRNA to travel actively along cytoskeletal filaments to these pre-disposed sites, where Ire1 concentrates.

Clustering of activated signaling receptors occurs in many systems, such as the immunological synapse25 and in bacterial chemotaxis26, and the resulting local concentration of the signaling machinery can profoundly enhance the efficiency of signal transduction. Interestingly, we found that upon oligomerization *in vitro* the nuclease activity of the Ire1 kinase/nuclease domains vastly increases over the activity observed for Ire1 dimers27 (AVK & PW, *submitted*). Thus, by clustering into oligomers, Ire1 acquires enhanced avidity towards its substrate *HAC1* mRNA and reaches full enzymatic activation at the same time. These mechanistic features converge into a signaling relay that provides the efficiency and timeliness required to combat ER stress.

METHODS SUMMARY

Microscopy data acquisition and analysis

Cells were visualized on a Yokogawa CSU-22 spinning disc confocal on a Nikon TE2000 microscope. Images of Ire1-mCherry and U1A-GFP decorated *HAC1*^{U1A}, SpR^{U1A} and *PGK1*^{U1A} mRNAs and variants thereof were analyzed using a customized MatLab script to determine the fraction of Ire1-mCherry in foci and to score the recruitment of U1A-GFP decorated mRNA in Ire1 foci. The annotated MatLab script is available in the Supplementary Material. In brief, after background subtraction we defined the fraction of Ire1-mCherry in foci as the ratio between the integrated fluorescence intensity of pixels with a signal greater than a threshold value and the total integrated fluorescence intensity. The threshold was empirically defined such that under non-stress conditions no signal was scored as “foci”. Similarly, RNA foci were defined as pixels exceeding twofold the mean intensity in the RNA channel. A “co-localization index” was then defined as the integrated intensity of the pixels within the RNA foci that had pixels in common with Ire1 foci divided by the total RNA intensity and expressed in arbitrary units in a range of 0 to 100. Per condition, the percentage of Ire1-mCherry in foci and the co-localization index for the mRNA recruited to the foci was determined for 3–9 individual cells. Values and the standard error of the mean are given in histograms in Figure 2–Figure 4. Since, in contrast to the covalently fluorescently tagged Ire1, we do not know what fraction of U1A-GFP is bound to mRNAs containing U1A binding sites, background subtraction for U1A-GFP was arbitrary. Therefore, we quantified the data by the co-localization index rather an absolute % co-localization measure. The co-localization index robustly scores the differences in mRNA recruitment we observed qualitatively in the fluorescent micrographs.

Full Methods and any associated references are available in the online version of the paper at www.nature.com/nature.

Supplementary Material

Refer to Web version on PubMed Central for supplementary material.

Acknowledgements

We thank Martin Jonikas and Benoît Kornmann for their help with the MatLab scripts; Roy Parker for the pPS2037 and pRP1187 plasmids; Kurt Thorn for the pKT127 plasmid and for his invaluable assistance with microscopy at the Nikon Imaging Center at UCSF; and Christine Guthrie, Raúl Andino, John Gross, and Walter lab members for discussion and comments on the manuscript. T.A. was supported by the Basque Foundation for Science and the Howard Hughes Medical Institute; E.v.A. by the Netherlands Organization for Scientific Research (NWO); D.P. and C.R. by the National Science Foundation; C.R. by the President’s Dissertation Year Fellowship; A.V.K. by the Jane Childs Memorial Fund for Medical Research. P.W. is an Investigator of the Howard Hughes Medical Institute.

References

1. Bernales S, Papa FR, Walter P. Intracellular signaling by the unfolded protein response. Annu. Rev. Cell Dev. Biol. 2006; 22:487–508. [PubMed: 16822172]
2. Ron D, Walter P. Signal integration in the endoplasmic reticulum unfolded protein response. Nat. Rev. Mol. Cell Biol. 2007; 8:519–529. [PubMed: 17565364]
3. van Anken E, Braakman I. Endoplasmic reticulum stress and the making of a professional secretory cell. Crit. Rev. Biochem. Mol. Biol. 2005; 40:269–283. [PubMed: 16257827]

4. Rüegsegger U, Leber JH, Walter P. Block of *HAC1* mRNA translation by long-range base pairing is released by cytoplasmic splicing upon induction of the unfolded protein response. Cell. 2001; 107:103–114. [PubMed: 11595189]
5. Sidrauski C, Cox JS, Walter P. tRNA ligase is required for regulated mRNA splicing in the unfolded protein response. Cell. 1996; 87:405–413. [PubMed: 8898194]
6. Sidrauski C, Walter P. The transmembrane kinase Ire1p is a site-specific endonuclease that initiates mRNA splicing in the unfolded protein response. Cell. 1997; 90:1031–1039. [PubMed: 9323131]
7. Travers KJ, et al. Functional and genomic analyses reveal an essential coordination between the unfolded protein response and ER-associated degradation. Cell. 2000; 101:249–258. [PubMed: 10847680]
8. Gonzalez TN, Sidrauski C, Dörfler S, Walter P. Mechanism of non-spliceosomal mRNA splicing in the unfolded protein response pathway. EMBO J. 1999; 18:3119–3132. [PubMed: 10357823]
9. Diehn M, Eisen MB, Botstein D, Brown PO. Large-scale identification of secreted and membrane-associated gene products using DNA microarrays. Nat. Genet. 2000; 25:58–62. [PubMed: 10802657]
10. Kimata Y, et al. Two regulatory steps of ER-stress sensor Ire1 involving its cluster formation and interaction with unfolded proteins. J. Cell Biol. 2007; 179:75–86. [PubMed: 17923530]
11. Brengues M, Teixeira D, Parker R. Movement of eukaryotic mRNAs between polysomes and cytoplasmic processing bodies. Science. 2005; 310:486–489. [PubMed: 16141371]
12. Teixeira D, Parker R. Analysis of P-body assembly in Saccharomyces cerevisiae. Mol. Biol. Cell. 2007; 18:2274–2287. [PubMed: 17429074]
13. Ghaemmaghami S, et al. Global analysis of protein expression in yeast. Nature. 2003; 425:737–741. [PubMed: 14562106]
14. Credle JJ, Finer-Moore JS, Papa FR, Stroud RM, Walter P. On the mechanism of sensing unfolded protein in the endoplasmic reticulum. Proc. Natl Acad. Sci. USA. 2005; 102:18773–18784. [PubMed: 16365312]
15. Pollock R, Rivera VM. Regulation of gene expression with synthetic dimerizers. Methods Enzymol. 1999; 306:263–281. [PubMed: 10432459]
16. Chartrand P, Meng XH, Huttelmaier S, Donato D, Singer RH. Asymmetric sorting of ash1p in yeast results from inhibition of translation by localization elements in the mRNA. Mol. Cell. 2002; 10:1319–1330. [PubMed: 12504008]
17. Anderson P, Kedersha N. RNA granules. J. Cell Biol. 2006; 172:803–808. [PubMed: 16520386]
18. Parker R, Sheth U. P bodies and the control of mRNA translation and degradation. Mol. Cell. 2007; 25:635–646. [PubMed: 17349952]
19. Kindler S, Wang H, Richter D, Tiedge H. RNA transport and local control of translation. Annu. Rev. Cell Dev. Biol. 2005; 21:223–245. [PubMed: 16212494]
20. Choi SB, et al. Messenger RNA targeting of rice seed storage proteins to specific ER subdomains. Nature. 2000; 407:765–767. [PubMed: 11048726]
21. Takizawa PA, DeRisi JL, Wilhelm JE, Vale RD. Plasma membrane compartmentalization in yeast by messenger RNA transport and a septin diffusion barrier. Science. 2000; 290:341–344. [PubMed: 11030653]
22. Czaplinski K, Singer RH. Pathways for mRNA localization in the cytoplasm. Trends Biochem. Sci. 2006; 31:687–693. [PubMed: 17084632]
23. Harding HP, Zhang Y, Ron D. Protein translation and folding are coupled by an endoplasmic-reticulum-resident kinase. Nature. 1999; 397:271–274. [PubMed: 9930704]
24. Shamu CE, Walter P. Oligomerization and phosphorylation of the Ire1p kinase during intracellular signaling from the endoplasmic reticulum to the nucleus. EMBO J. 1996; 15:3028–3039. [PubMed: 8670804]
25. Bromley SK, et al. The immunological synapse. Annu. Rev. Immunol. 2001; 19:375–396. [PubMed: 11244041]
26. Maddock JR, Shapiro L. Polar location of the chemoreceptor complex in the Escherichia coli cell. Science. 1993; 259:1717–1723. [PubMed: 8456299]

27. Lee KP, et al. Structure of the dual enzyme Ire1 reveals the basis for catalysis and regulation in nonconventional RNA splicing. Cell. 2008; 132:89–100. [PubMed: 18191223]

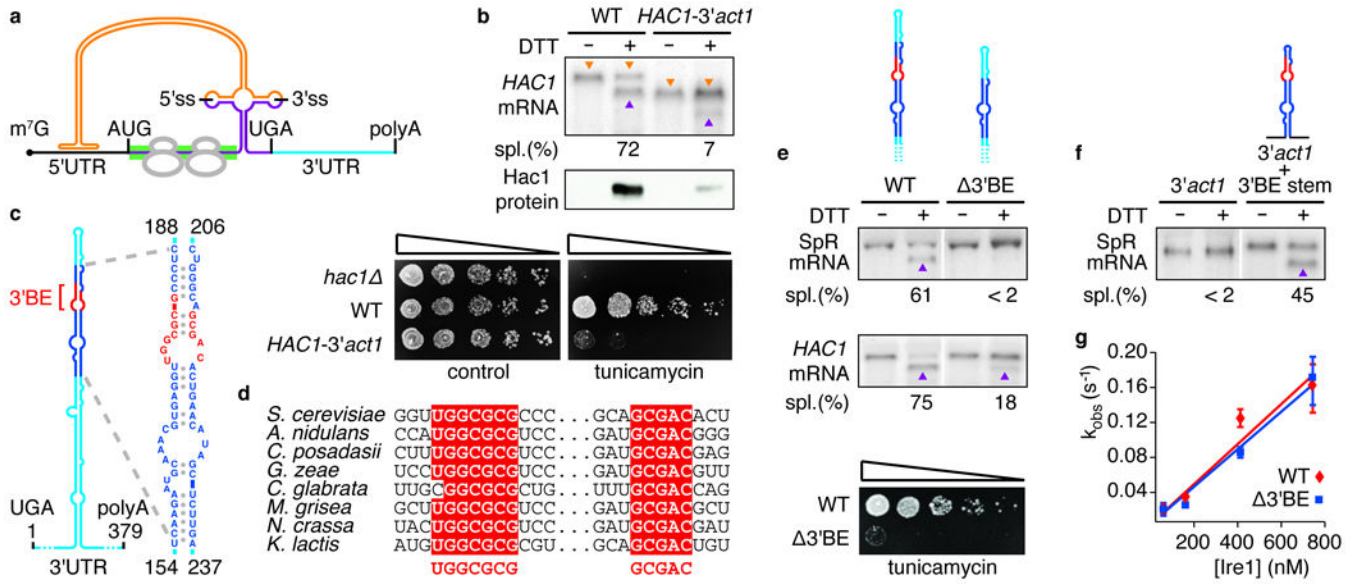

Figure 1. A conserved element in the 3'UTR of *HAC1* mRNA is required for splicing *in vivo*, but not *in vitro*

a, Schematic of *HAC1* mRNA. The Hac1 ORF is divided into two exons (purple). The intron (orange) base pairs with the 5′UTR (black), causing ribosome stalling (grey). Ire1 cleaves the intron at the indicated splice sites (5′ss & 3′ss). The green bar depicts where the GFP ORF replaces the *HAC1* sequence in the splicing reporter. The 3′UTR is indicated in light blue. The 5′cap (m^7G), start codon (AUG), stop codon (UGA) and polyadenylation signal (polyA) are indicated. **b**, **e, f**, Northern blot of *HAC1* or SpR mRNA variants before or after ER stress induction with DTT (10 mM) for 45 min. Purple triangles denote spliced mRNAs; orange triangles denote unspliced mRNAs (only in **b**). Percent mRNA splicing ("Spl. (%)") is indicated. Yeast strains harbor a genomic *HAC1* copy with its own (WT) or *ACT1*'s 3′UTR sequence (*HAC1*-3′*act1*) (**b**, top), a genomic copy of SpR (**e**, top) or *HAC1* (**e**, middle) bearing either the wild-type (WT) or the Δ3′BE mutant 3′UTR, as depicted, or a genomic copy of SpR with the 3'UTR of *ACT1* with (3′*act1*+3′BE stem) or without (3′*act1*) an insertion of the 64 nucleotide element — shown in expanded view in (**c**) — as depicted (**f**). **b**, middle, Western blot of HA-tagged Hac1 protein from lysates from strains as in (**b**, top). **b**,**e**, Viability assay by 1:5 serial dilutions of *hac1*Δ or strains as in (**b**, top) or (**e**, middle) spotted onto solid media with or without 0.2 μg/ml of the ER stress inducer tunicamycin. Plates were photographed after 3 days growing at 30°C. **c**, Schematic of the *HAC1* 3′UTR stem-loop structure with the 3'BE (red) in a region (dark blue) that is shown in expanded view to the right; positional numbering from UGA stop codon. **d**, alignment of the 3′BE in *HAC1* homologues. **g**, An *in vitro* intron excision reaction was performed as described8 with Ire1 concentrations: 50 nM, 150 nM, 400 nM, 730 nM of wild-type (red diamonds) or Δ3′BE (blue squares) *HAC1* mRNA as substrates.

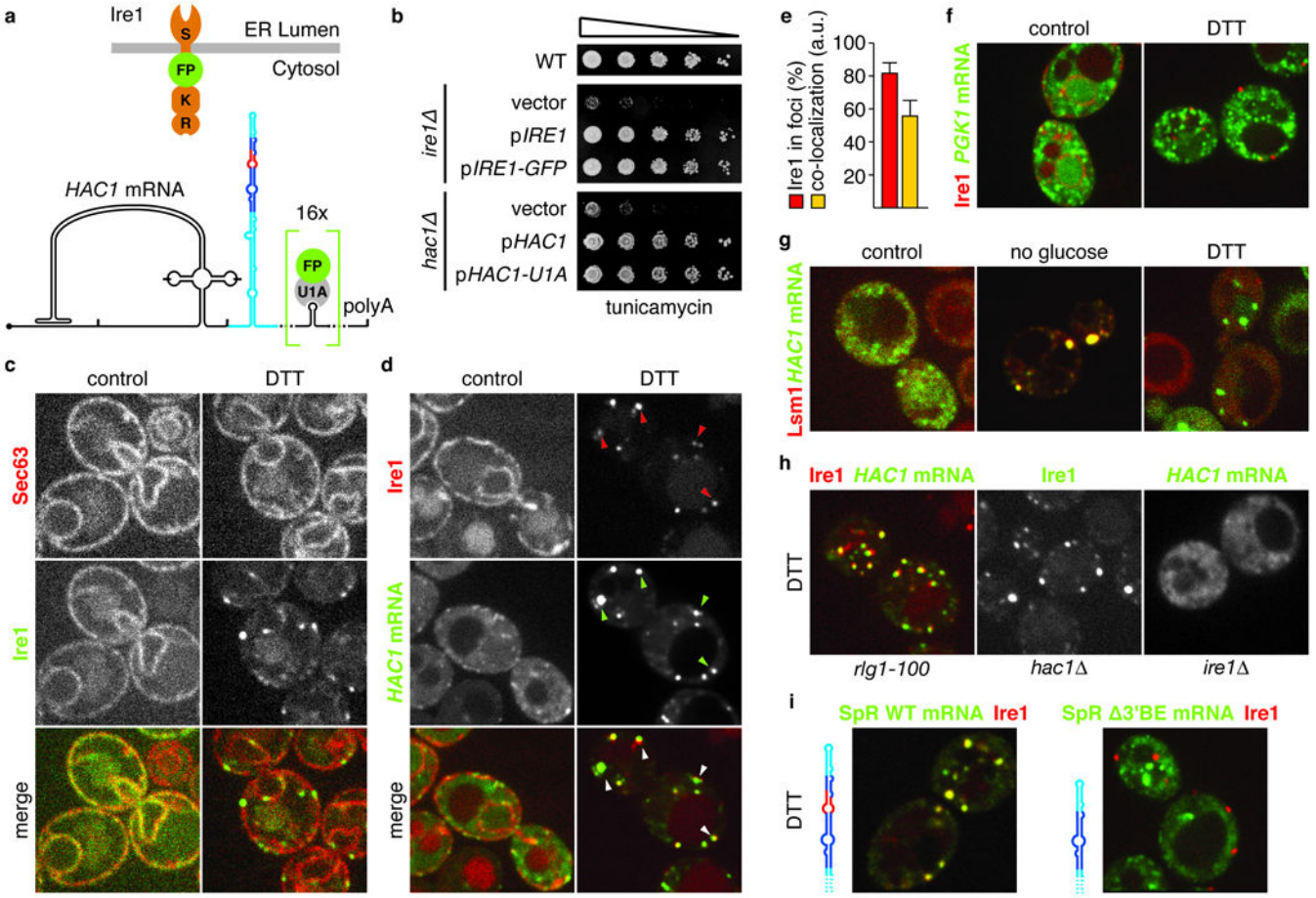

Figure 2. In response to ER stress *HAC1* mRNA localizes to Ire1 foci in a 3'BE-dependent manner

a, Schematic of Ire1 and *HAC1* mRNA imaging constructs: Ire1 has an ER-luminal stress sensing domain (S) and a kinase (K) and endonuclease domain (E) at its cytosolic face. GFP or mCherry (FP) was inserted between the transmembrane region and the kinase domain (up). **b**, Viability assay under ER stress conditions (0.2 μg/ml tunicamycin) of wild-type or *ire1*Δ yeast complemented with either empty vector, or centromeric plasmids bearing a wild-type (pIRE1), or the GFP-tagged imaging copy of Ire1 (pIRE1-GFP) (top) or *hac1*Δ yeast complemented with either empty plasmid, or a 2-micron plasmid bearing a wild-type (pHAC1) or the U1A-tagged imaging copy of *HAC1* (pHAC1-U1A) (bottom). **c**,**d**, Localization of Sec63-mCherry and Ire1-GFP (**c**) or Ire1-mCherry and *HAC1*^{U1A} mRNA decorated with U1A-GFP (**d**) before (left panels, control) and after (right panels, DTT) induction of ER stress. Arrowheads in **d**, lower panels, denote Ire1/*HAC1* mRNA foci. **e**, Histogram depicting the percentage of Ire1 signal in foci (red bar) and the C.I. for *HAC1*^{U1A} mRNA recruitment into Ire1 foci expressed in arbitrary units ("a.u.", yellow bar); means +/− s.e.m., n = 9. **f**, Localization of Ire1-mCherry and *PGK1*^{U1A} mRNA decorated with U1A-GFP under normal (left panel, control) and ER stress (right panel, DTT) conditions. **g**, Localization of Lsm1-mCherry and *HAC1*^{U1A} mRNA without stress (left panel, control), after nutrient starvation for 10 min (middle panel, no glucose), or after induction of ER stress (right panel, DTT). **h**,**i**, Localization of Ire1-mCherry, Ire1-GFP, or *HAC1*^{U1A} or SpR

having 16 U1A hairpins as *HAC1*^{U1A} (SpR^{U1A}) either with or without the Δ3′BE deletion after induction of ER stress (DTT). **c–i**, ER stress was induced with 10 mM DTT for 45 min; imaging was performed in *ire1*Δ cells, complemented with Ire1 imaging constructs, except in (h) cell were *hac1*Δ or *rlg1-100*.

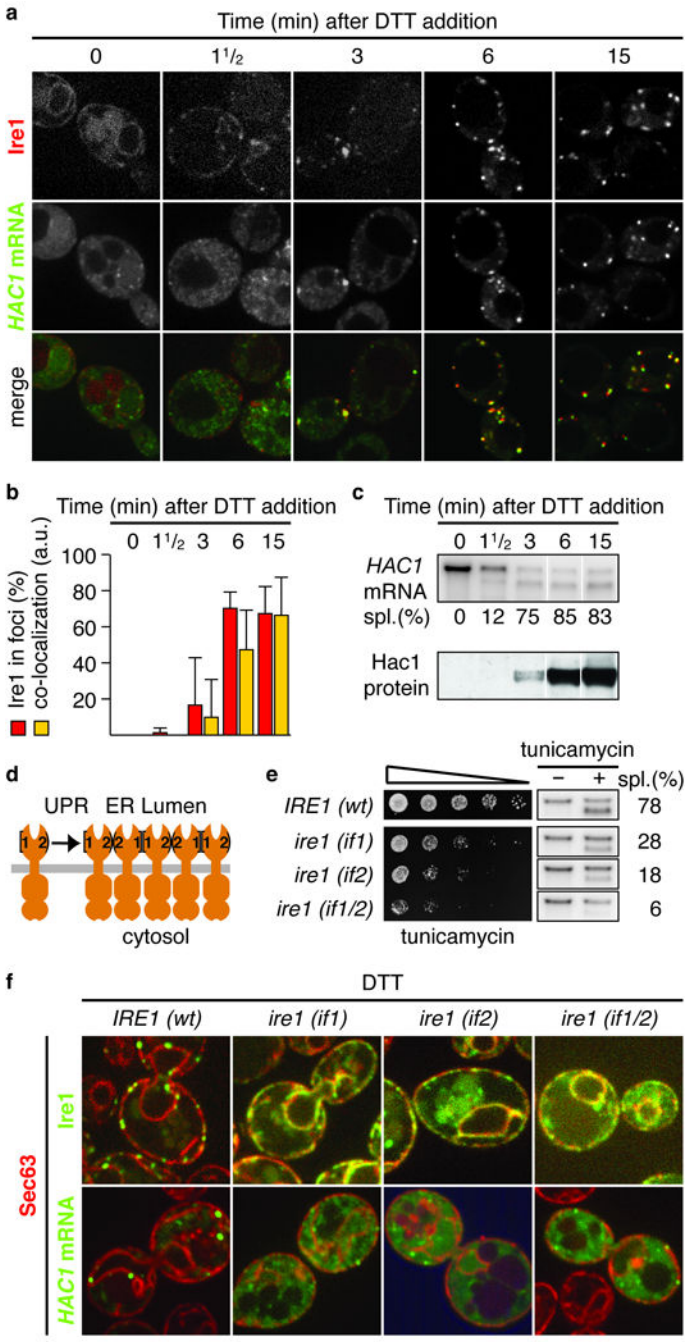

Figure 3. The *HAC1* mRNA/Ire1 foci are functional UPR signaling centers

a, Localization of Ire1-mCherry and *HAC1*^{U1A} mRNA decorated with U1A-GFP. **b**, Quantitation of the percentage of Ire1 signal in foci (red bars) and of the C.I. for *HAC1*^{U1A} mRNA recruitment into Ire1 foci (yellow bars; means +/− s.e.m., n = 5). **c**, Northern blot of *HAC1* mRNA (top) and Western blot of Hac1 protein (bottom). **a–c**, Samples were taken at indicated times after induction of ER stress with 10 mM DTT. **d**, Schematic of Ire1 oligomerization via interfaces 1 and 2. **e**, Viability assay under ER stress conditions (0.2 μg/ml tunicamycin) and Northern blot of *HAC1* mRNA harvested from *ire1*Δ yeast

complemented with wild-type Ire1 or interface mutants before or after treatment with 1 μg/ml tunicamycin for 1 h. **f**, Localization of Sec63-mCherry, Ire1-GFP, and *HAC1*^{U1A} mRNA. Imaging was performed in *ire1*Δ yeast complemented with wild type or mutants of Ire1 that are defective in dimarization at interface 1 (*if1*), 2 (*if2*) or both (*if1/2*), either GFP-tagged (top) or untagged (bottom). ER stress was induced: 10 mM DTT 45 min. Separate channels are displayed in Supplementary Fig. S3.

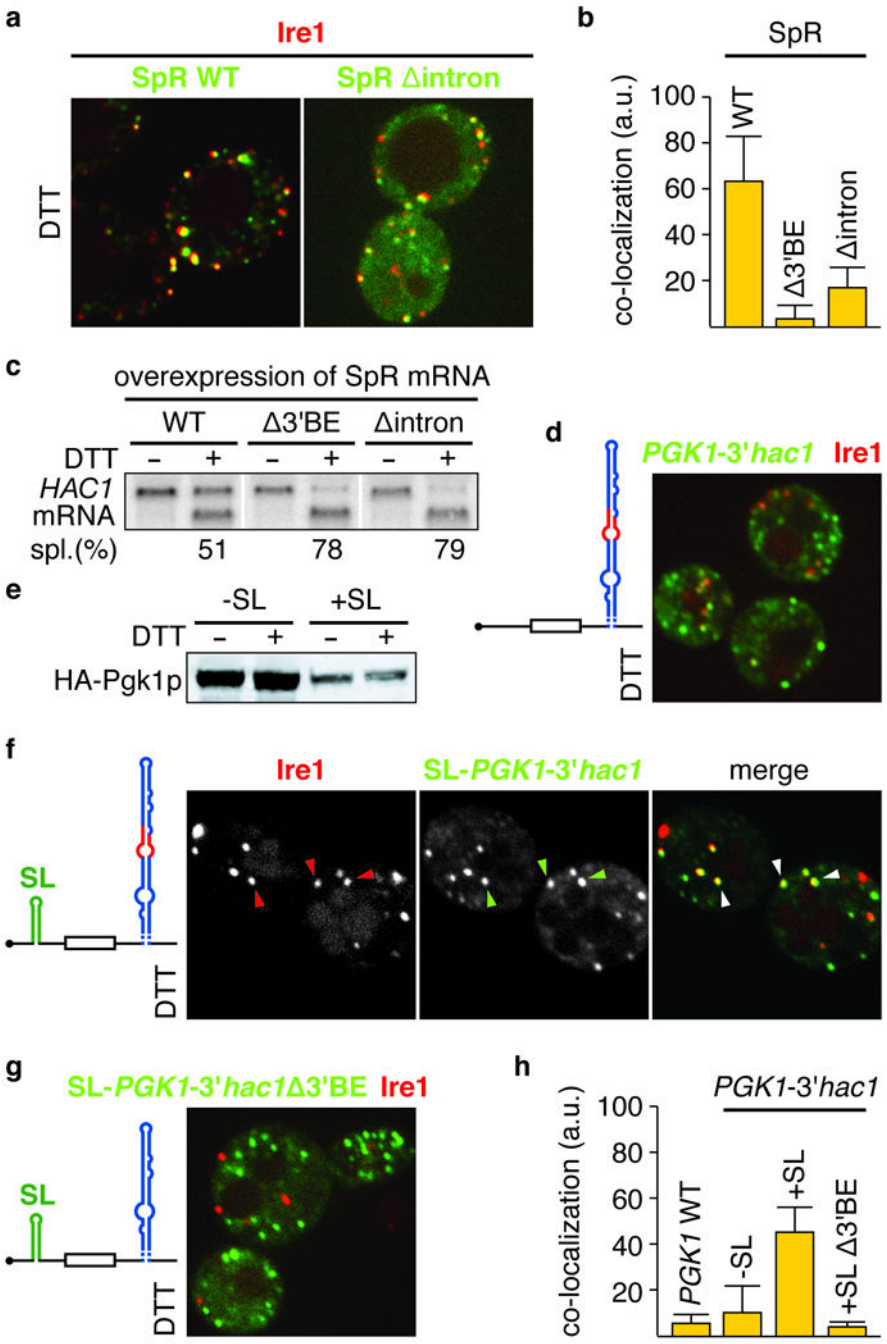

Figure 4. Translational repression is a prerequisite for mRNA targeting to Ire1 foci

a,d,f–g, Localization of Ire1-mCherry, and U1A-GFP decorated mRNA of either the wild-type splicing reporter, as in Figure 2i (SpR WT), or an intron-less variant (SpR Δintron) (**a**), or of *PGK1*^{U1A}, bearing either the wild-type (**d,f**) or mutant Δ3′BE (**g**) 3′UTR stem loop of *HAC1* mRNA, in combination with (**f,g**) or without (**d**) a small stem loop (SL) that confers translational repression in its 5′UTR, as schematically depicted. **b**, C.I for mRNA recruitment of WT and Δintron SpR variants into Ire1 foci (means +/− s.e.m., n = 5); bar for the Δ3′BE mutant as depicted in Figure 2i is shown for comparison. **c**, Northern blot of

HAC1 mRNA from yeast strains that over-expressed variants of the SpR, as indicated. **e**, Western blot of the variants of HA-tagged Pgk1 protein (HA-Pgk1p) bearing the 3′UTR from *HAC1* with or without a 5′UTR SL **a,c–g**, ER stress was induced with 10 mM DTT for 45 min. **h**, C.I. for mRNA recruitment into Ire1 foci of *PGK1*^{U1A} wild-type — see Figure 2f — or variants shown in **d,f,g** (means +/− s.e.m., n = 3–5).